MODELING OF POLYURETHANE FOAM THERMAL DEGRADATION WITHIN AN ANNULAR REGION SUBJECT TO FIRE CONDITIONS

[1]Miles Greiner, [2]Jie Li, [2]Shiu-Wing Tam, [2]Yung Liu, and [3]Allen Smith

[1]University of Nevada, Reno, NV, USA, greiner@unr.edu
[2]Argonne National Laboratory, Argonne, IL, USA
[3]Savannah River National Laboratory, Aiken, SC, USA

ABSTRACT

Nuclear materials are placed in shielded, stainless-steel packaging for storage or transport. These drum-type packages often employ a layer of foam, honeycomb, wood, or cement that is sandwiched between thin metal shells to provide impact and thermal protection during the hypothetical accidents, as those prescribed in the Code of Federal Regulations (10 CFR 71.73), to provide impact and thermal protection during hypothetical accidents. This work discusses the modeling of the thermal degradation of a polyurethane foam within an annular region during an 800°C fire. Measurements and analysis by Hobbs and Lemmon [in *Polymer Degradation and Stability*, Vol. 84, pp. 183–197, 2004] indicate that at elevated temperatures, polyurethane foam exhibits a two-stage, endothermic degradation. The first stage produces a degraded solid and a combustible gas; the second-stage reaction consumes the degraded solid and produces another combustible gas. As a result, during a prolonged fire a gas-filled void develops adjacent to the outer metal shell and grows inward toward the inner shell and the containment vessel.

As a result of radial symmetry in the drum geometry, a one-dimensional finite-difference model is constructed for the annular foam region. Heat flux is applied to the inner surface to model the decay heat of the containment vessel contents. Thermal radiation and convection boundary conditions with a specified environmental temperature are applied to the outer surface. The material and reaction rate properties determined by Hobbs and Lemmon are applied to the foam. The annular region temperature and composition are determined as functions of radius and time, after the environmental conditions are changed from room temperature to those of an 800°C fire. The effects of surface-to-surface radiation between the package's outer skin and the un-degraded foam, the reaction rate reduction due to material damage during the reaction, are evaluated for fires lasting 20 hours. The peak package liner temperature caused by a 30-minute fire is predicted to be 129°C, well below the short-term limit for the containment vessel seal (377°C).

INTRODUCTION

Packages that transport large quantities of nuclear materials must be qualified to withstand a series of regulatory tests. These tests include a 9-m drop or a crush test, a 1-m drop onto a steel puncture bar, and full engulfment in an 800°C fire for 30 minutes [1]. Polyurethane (PU) foams

are used in the impact limiters of fuel packages [2] and in other exterior regions of drum packages [3] because of their ability to absorb energy during impacts and insulate the package during fires [4].

Figure 1 shows a cutaway of a 9977 general-purpose fissile package [3]. At its center is a containment vessel and load distribution fixtures within a cylindrical liner assembly. The liner is made from 1.22 mm (0.048 in.) thick, 18-gage 304L stainless steel with an inner diameter of 20.96 cm (8.25 in.). Two 1.27-cm (0.5-in.) thick Fiberfrax® blankets are wrapped around the sides and bottom of the liner. The package outer skin is also made from 18-gage 304L stainless steel. The radial distance between the exterior surface of the liner and the interior surface of the skin is 12.57 cm (4.95 in.). The space between the Fiberfrax® and the outer skin is filled with General Plastics FR-3716 PU foam with a density of 0.26 kg/cm^3 (16 lbm /ft^3). When the package is in use, a cover with a plug assembly is bolted on the package. The distance between the bottom of the plug and the bottom of the liner is 63.0 cm (24.81 in.). There are 12 holes with a diameter of 1.91 cm (0.75 in.) on the package sides, and there are two more two holes on the bottom to vent hot material out of the overpack during a fire.

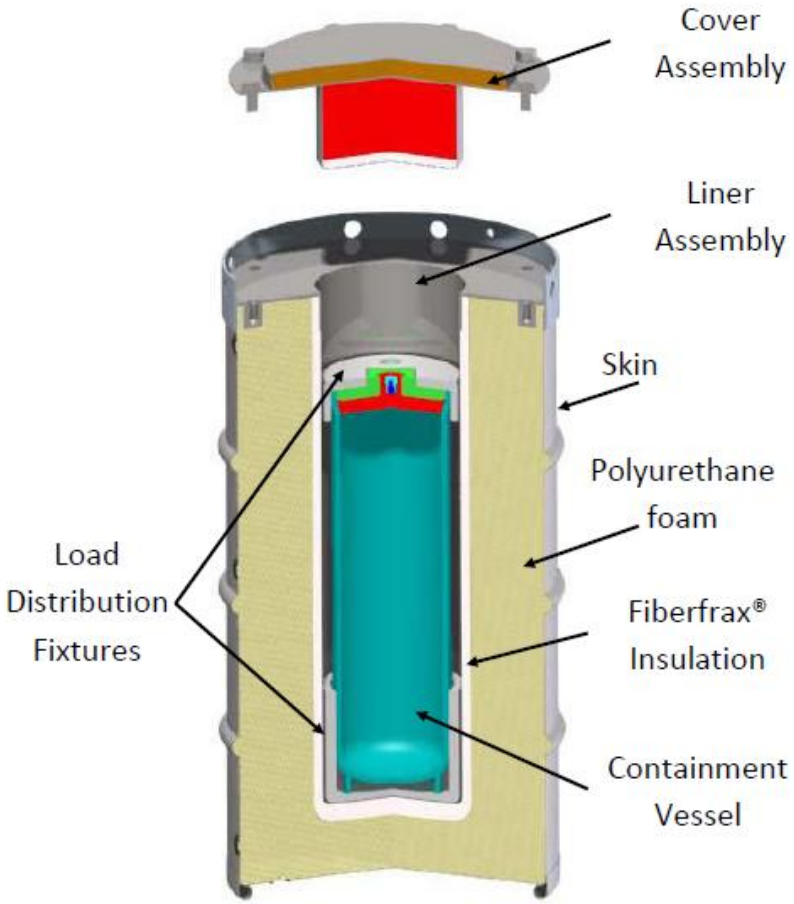

Figure 1 Cutaway of a 9977 package, including a containment vessel inside the liner assembly.

For the 9977 package to operate satisfactorily, the containment vessel seal temperature must be below 204°C (477K, 400°F) during normal conditions and 377°C (650K, 700°F) during or after a regulatory fire. The thermal behavior of the PU foam at high temperatures is complex, which makes it difficult to accurately predict heat transfer though the foam and the resulting seal temperature. The objective of the current work is to develop a model for this behavior and the resulting heat transfer.

The behavior of PU foam under high-temperature conditions depends on the presence of an oxidizer [5]. The foam is combustible in the presence of an oxidizer. In the absence of oxygen, it reacts by endothermic pyrolysis. This reaction produces degraded solid products and gases that are combustible in the presence of oxygen.

Figure 2 shows mocked-up 9977 packages shortly after they were removed from high-temperature fire and oven environments [6,7]. Figure 2a shows high-temperature flairs jetting out of holes in the package skin. These flairs can continue to burn several minutes after the package is removed from the hot environment. Figure 2b shows large volumes of charred foam product after it was emitted from holes in the sides of the package. This product essentially disappears after a few hours when it is exposed to air in a moderately-high-temperature environment (such as an oven while it is cooling down after a high-temperature test).

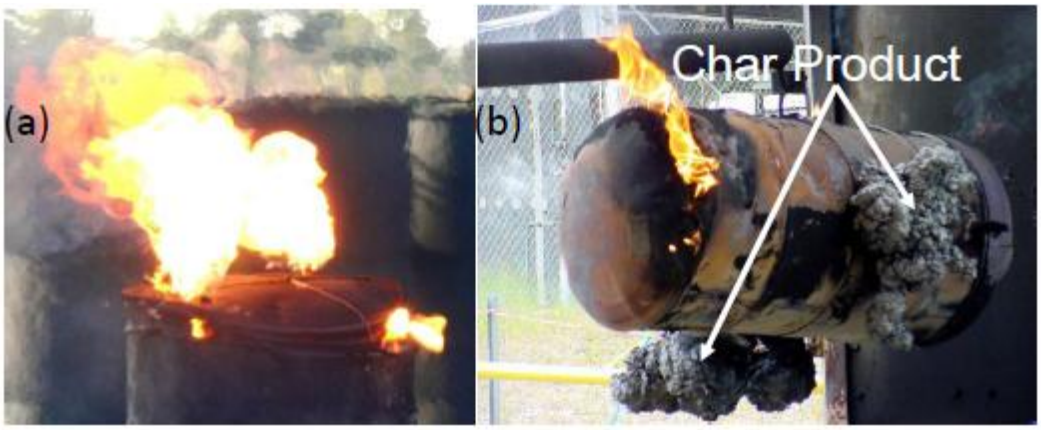

Figure 2 Polyurethane foam reaction products emitted from 9977 shortly after exposure to high-temperature environments. (a) Jetting flames (b) Char product and lower-speed flames

Figure 3 shows pictures of a 9977 package after it was subjected to Code of Federal Regulations (10 CFR Part 71) crush, puncture, and fire testing. Figure 3a shows a radiograph. The package skin is deformed from the crush and puncture tests. The liner and cover are the darkest areas because they are the densest regions. Close examination of the picture shows there are two levels of darkness between the liner and skin. The darker region near the liner is the more dense PUfoam that did not react during the fire. The lighter region is the less dense char product that was produced during the fire. Figure 3b is a picture of the same package with part of the stainless-steel skin removed. The charred foam product is very fragile and porous and exhibits a nodular and channeled morphology. Figure 3c shows the un-degraded foam after the char product was chipped away.

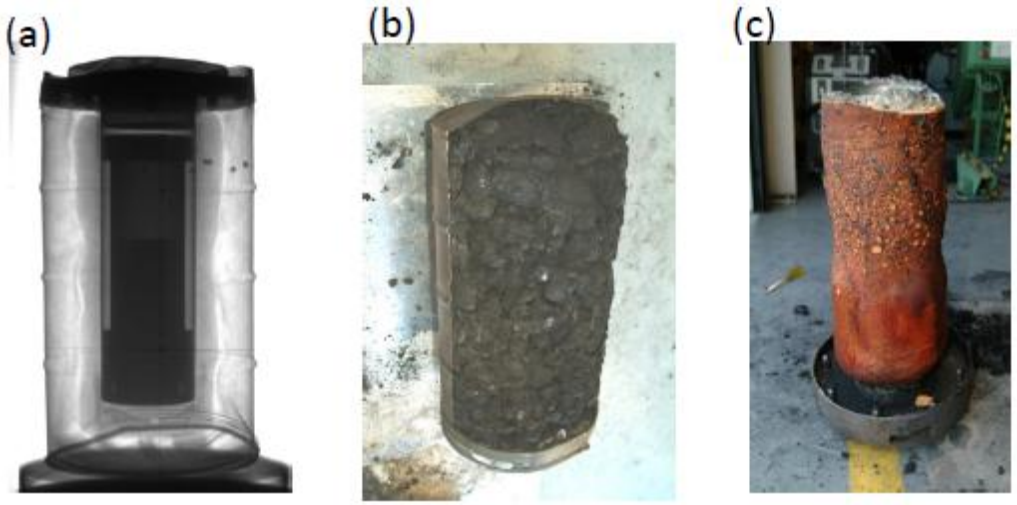

Figure 3 Pictures of a 9977 package after regulatory crush, puncture, and fire tests. (a) Radiograph. (b) Char product after skin has been removed. (c) Un-degraded polyurethane foam after char product was removed.

In the current work, we hypothesize the following physical mechanism for the thermal degradation of the PU foam on the basis of these experimental observations. When the package is first placed in a fire environment, the PU foam outer layers heat up. When the foam is sufficiently hot, it degrades by pyrolysis because there is limited oxygen within the package skin. The process produces a combustible gas as well as a melted viscous material. As the gas expands and mixes with the viscous material, the mixture forms an intumescent material that first fills the volume vacated by the PU foam, and then flows out of holes in the package skin. The high-temperature region moves toward the package center as the fire continues, and the reaction front moves with it. If the fire lasts long enough all of the foam will react. During the process, gas generated within the PU foam flows outward toward the package skin, carrying energy with it. When it exits through holes in the side of the packages, it is able to mix with air and combust.

In this paper, we develop a one-dimensional model of PU foam thermal degradation within an annular region subjected to external fire conditions. This region is similar to the region between the liner and outer skin of a 9977 package. We model a two-step thermal degradation reaction. The rate of both steps is governed by an Arrhenius temperature dependence. Here, we reduce the rates when a significant fraction of the foam has been reacted to account for cumulative chemical and mechanical damage to the foam material. We employ different damage models to find one that includes residual char or degraded solid between the un-degraded foam and the package skin, similar to that observed in Figure 3.

The thermal model used in this work includes the effect of radiation and convection between a normal or fire environment and the external surface of the package skin. It calculates transient conduction in the skin, liner, and the region between the skin and liner that contains foam and gas products. It also includes consumption of the PU foam, generation of heat and char and gas

products, and mixture material properties based on the local mass and volume fraction of the solid and gas components. Radiation from the interior surface of the package skin to the exterior surface of the un-degraded foam is modeled when the degraded foam has been sufficiently consumed that it has essentially been replaced by non-participating gas. This model does not include the effect of the product gas flowing though the degraded PU foam or the flow of intumescent char product. These effects may be addressed in future work.

THERMAL DEGRADATION KINETICS MODEL

Hobbs and Lemmon [8, 9] developed a kinetics model for thermal degradation of PU foam. It is a simplified version of more general models they developed earlier, and it is valid for unconfined foams at atmospheric pressure. This simplified polyurethane foam response (SPUR) model involves four components: the un-degraded foam, a degraded solid, a primary product gas, and a secondary product gas. They analyzed thermo-gravimetric measurements of a foam sample to determine that thermal degradation involves two reaction steps. The mass-based reaction steps are

$$F \rightarrow 0.7\ G_1 + 0.3\ S \qquad \text{(reaction rate } r_1\text{)} \qquad (1)$$

$$S \rightarrow G_2 \qquad \text{(reaction rate } r_2\text{)} \qquad (2)$$

In these expressions, F, G_1, S, and G_2 are dimensionless mass-based progress variables. They are, respectively, the masses of the foam, primary gas, degraded solid, and secondary gas divided by the initial mass of the foam $m_{Foam,0}$ ($F = m_{Foam}/m_{Foam,0}$, $G_1 = m_{G1}/m_{Foam,0}$, $S = m_S/m_{Foam,0}$, $G_2 = m_{G2}/m_{Foam,0}$). Before the reaction begins, F = 1 and $G_1 = S = G_2 = 0$. After a sufficiently long-duration thermal degradation process, both solids are consumed so F = S = 0, and the two gases are produced such that $G_1 = 0.7$ and $G_2 = 0.3$. During this long process, S first increases to a positive value and then decreases back to zero. In shorter-duration fires that do not consume all of the foam, the final values of F, S, G_1, and G_2 are different.

The reaction rates of the two steps r_1 and r_2 have units of kg/(kg s). Both reactions steps are endothermic, with equal volumetric heats of reaction $h_{r1} = h_{r2} = -29.2$ cal/cm^3 = -122 MJ/m^3. The SPUR model uses the following normally-distributed Arrhenius reaction rates:

$$r_1 = F * A * \exp[-(E_1+z_1\sigma_1)/RT] \qquad (3)$$

$$r_2 = S * A * \exp[-(E_2 + z_2\sigma_2)/RT] \qquad (4)$$

In these expressions, the pre-exponential constant is $A = 10^{13}$ 1/s, the universal gas constant is R = 1.9859 cal/mol K, and the local temperature is T. The mean activation energies for the two reactions are $E_1 = 41.4$ kcal/mol and $E_2 = 45.1$ kcal/mol.

The mean of the distribution parameters for the two reactions are $\sigma_1 = 1.08$ kcal/mol and $\sigma_2 = 3.14$ kcal/mol. They are used to model the reduction in the reaction rate caused by cracks and thermal decomposition in the reactants that accumulate during the reaction. The distribution variables for reactions 1 and 2, z_1 and z_2, increase with the extent of those reactions, $\Phi_1 = 1 - F$ and $\Phi_2 = 1-(F+S)$. At the beginning of the reaction the extents are $\Phi_1 = \Phi_2 = 0$, and they

approach 1 as the reactions near completion. For normally-distributed reactions the relationships between the distribution variables z_1 and z_2 and the reaction extents are:

$$1-F=\Phi_1(z_1)=\int_{-\infty}^{z_1}\frac{1}{\sqrt{2\pi}}\exp(-\frac{1}{2}z^2)dz \qquad (5)$$

$$1-(F+S)=\Phi_2(z_2)=\int_{-\infty}^{z_2}\frac{1}{\sqrt{2\pi}}\exp(-\frac{1}{2}z^2)dz \qquad (6)$$

The distribution variables z_1 and z_2 are both infinitely large negative numbers at the beginning of the reactions since 1 – F = 1–(F+S) = 0. In Equations 3 and 4, this effectively reduces the activation energy compared to $\sigma_1 = \sigma_2 = 0$ which increases the reaction rates. As the reactions near completion, 1- F and 1–(F+S) both approach 1. As a result z_1 and z_2 become large positive numbers, which effectively retards the reactions.

The dependence of Φ on z for a normal-distribution may be found by numerical integration of Equations 5 or 6. The inverse of this relationship, $z = z_N(\Phi)$,is shown by the line marked "Normal" in Figure. 4 (the irregularities in the curve are caused by using a polynomial fit to the numerical data, and do not affect the results of this study). In the current work, the values of z are limited to $-4 \le z \le 10$. In the current calculations, the reaction extents $\Phi_1 = 1 - F$ and $\Phi_2 = 1 - (F+S)$ are calculated at each time and location within the computational domain. The distribution variables z are then determined from the data in Figure 4 and used in Equations 3 and 4 to find the reaction rates.

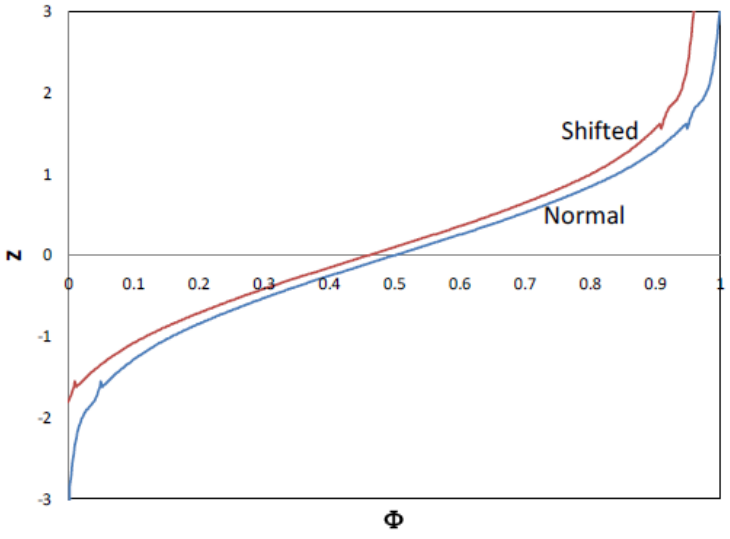

Figure 4 Distribution variable used in Equations 3 and 4 versus reaction completion based on normal and shifted damage models.

COMPUTATIONAL METHODS

Figure 5 shows the axis-symmetric model of the 9977 package cross section used in the current work. It includes the liner assembly and skin and a foam/gas region between them. The inner

diameters of the liner and skin are 20.96 cm (8.25 in) and 46.34 cm (18.25 in), respectively. The thicknesses of the liner and skin are both 1.22 mm (0.048 in). Initially, the region between the liner and skin is filled with PU foam (the Fiberfrax® insulation is neglected in the current model). After the reaction begins, there is a region near the skin with a low solid mass fraction (SMF), where solid foam has reacted and produced gas, and there is a high-SMF region near the liner. The low-SMF region grows toward the liner as the reaction continues. However, the current calculation does not model the flow of material. As a result, gas generated within any location in the domain remains at that location.

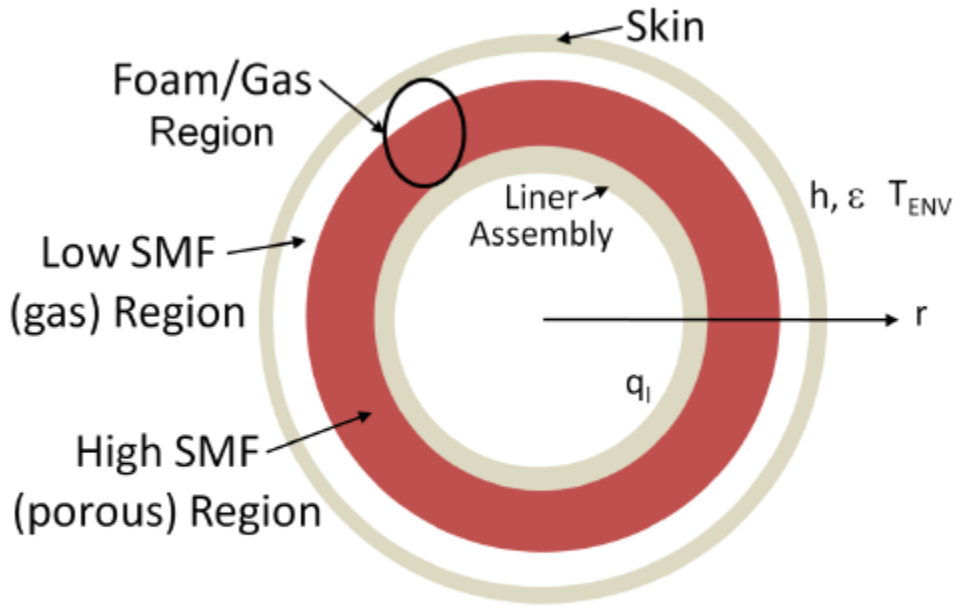

Figure 5 Regions of 9977 overpack cross section showing the liner assembly, package skin, and a foam/gas region with high and low solid mass fraction (SMF) areas.

The domain in Figure 5 is broken into concentric cylindrical control volumes, as shown in Figure 6. The liner and skin are each broken into two volumes, with node points (represented by dots) at the interior and exterior surfaces of those components. The foam/gas region was broken into N volumes with nodes at their centers. Figure 6 shows three volumes near the middle of that region, which are indexed as i –1, i and i+1. In this work we performed simulations with both N = 50 and N = 100, and the results were essentially the same. We wish to determine the temperature and composition at all the nodes as functions of location and time during and after fires of temperatures T_{FIRE} and durations D_{FIRE}.

Within each control volume *i*, the volume per unit length (normal to the plane of Figure. 6) is V_i. The radial distance from each node to the center of the domain is R_i. The mass per unit length of species j at time step t is $m_{i,j}^t$. The species subscripts j = 1, 2, 3, and 4 correspond to foam (F), primary product gas (G_1), degraded solid (S), and secondary product gas (G_2), respectively. For

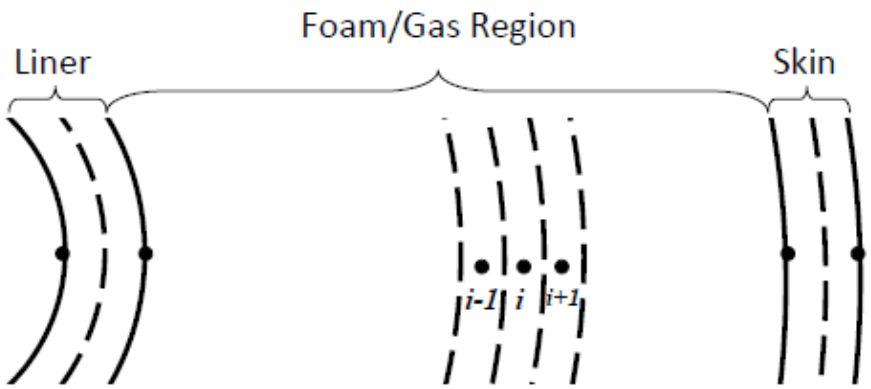

Figure 6 Structure of finite volumes and node points used in the axis symmetric calculation performed in the current work

a time step size Δt, we use an explicit form of conservation of species mass to calculate the change in each species-mass:

$$\frac{m_{i,1}^{t+1} - m_{i,1}^{t}}{\Delta t} = V_i(-r_1^t) \qquad (7)$$

$$\frac{m_{i,2}^{t+1} - m_{i,2}^{t}}{\Delta t} = V_i(0.7r_1^t) \qquad (8)$$

$$\frac{m_{i,3}^{t+1} - m_{i,3}^{t}}{\Delta t} = V_i(0.3r_1^t - r_2^t) \qquad (9)$$

$$\frac{m_{i,4}^{t+1} - m_{i,4}^{t}}{\Delta t} = V_i(r_2^t) \qquad (10)$$

where r_1^t and r_2^t are from the rate expressions, Equations. 3 and 4, evaluated at time t. Since this model does not include flow between control volumes, the total mass m_i and density ρ_i in each volume does not change with time. Future work will include flow of product gas through the porous media of the degraded foam [10].

In this work the solid mass fraction in any control volume is the mass of the solids, F and S, which correspond to j =1 and 3, divided by the total mass,

$$SMF_i^t = \frac{m_{i,1}^t + m_{i,3}^t}{m_{i,1}^t + m_{i,2}^t + m_{i,3}^t + m_{i,4}^t} \qquad (11)$$

We assume radiation heat transfer is able to be transmitted through control volumes whose solid mass fraction is $SMF_i < 0.038$ (Hobbs and Lemmon 2004).

The temperature at each node i and time step t is T_i^t. The explicit form of the conservation of energy constraint at node i is used to calculate the change in nodal temperature,

$$(\rho c_v)_i V_i \frac{T_i^{t+1} - T_i^t}{\Delta t} = 2\pi k_{i-1,i} \frac{T_{i-1}^t - T_i^t}{\ln(\frac{R_i}{R_{i-1}})} + 2\pi k_{i,i+1} \frac{T_{i+1}^t - T_i^t}{\ln(\frac{R_{i+1}}{R_i})} + V_i(H_1 r_1^t + H_2 r_2^t) + Q_{Rad}^t \quad (12)$$

In this expression, the term to the left of the equal sign is the rate of change of internal energy of the control volume. The first two terms on the right side represent conduction from the neighboring control volumes, i-1 and i+1. The next term calculates heat generation from the two reaction steps. The last term is for radiation heat transfer from the interior surface of the skin to the exterior surface of control volume i.

The volumetric specific heat at constant volume $(\rho c_v)_i$ is the density times the mass-based specific heat within *i*. In general, each control volume can contain all four components, j = 1, 2, 3, and 4. Hobbs and Lemmon [8,9] measured thermal properties of PU foams with different initial densities. The temperature-dependent thermal conductivity and mass-based specific heat for foam with an initial density of $\rho = 0.352$ gm/cm^3 is shown in Figures 7a and 7b, respectively. In the current work, we use these properties for both the un-degraded foam and the degraded solid. We use the properties of air for both the primary and secondary gas products (future work may use more realistic properties of carbon dioxide and steam mixtures). To determine the specific heat of the mixture of all four components within each control volume we use the conservation-of-energy-based expression

$$c_{v,i} = SMF_i \cdot c_{v,PU}(T_i) + (1 - SMF_i) \cdot c_{v,AIR}(T_i) \quad (13)$$

where $c_{v,PU}$ and $c_{v,Air}$ are the specific heats of PU foam and air, respectively.

The effective thermal conductivity of mixtures is dependent on the thermal conductivities of the components and the geometry of the components within the mixture. When a gas is one of the components, the radiative properties of the surfaces and gases are also involved. For simplicity, in the current work we assume that the cross-sectional areas of the components in the heat flow (radial) direction are uniform and that radiation heat transfer is not important. In that case, the mixture thermal conductivities depend on the solid *volume* fractions of each component [10]. The solid volume fraction is the volume of solid within the control volume divided by the total value

$$SVF_i = \frac{V_{i,F} + V_{i,S}}{V_i} = \frac{(m_{i,1} + m_{i,3})/\rho}{(m_{i,1} + m_{i,2} + m_{i,3} + m_{i,4})/\rho} \quad (14)$$

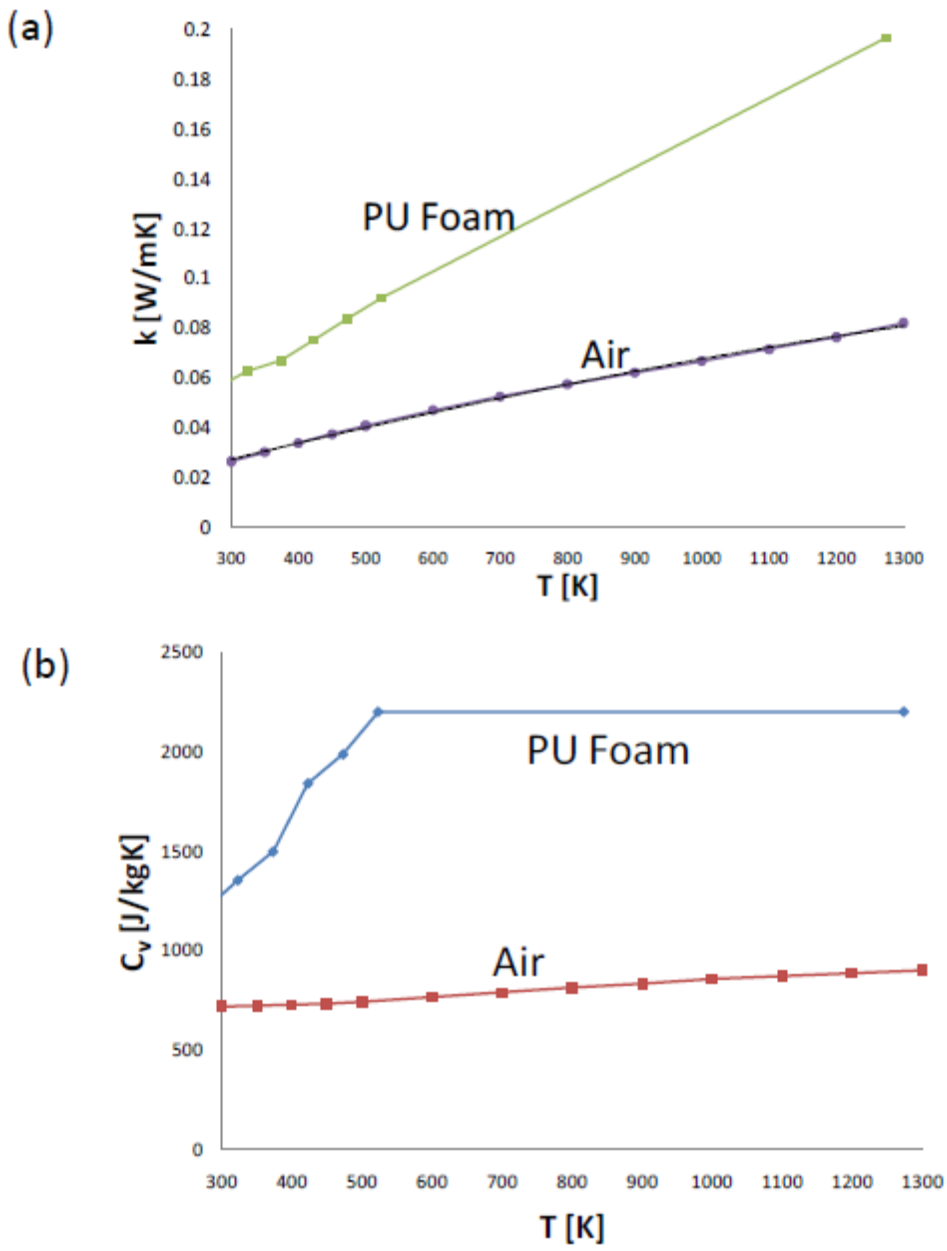

Figure 7 Temperature-dependent thermal properties of polyurethane (PU) foam [Hobbs and Lemmon 2004] and product gas (modeled as air). (a) Thermal conductivity. (b) Specific heat at constant volume

We note that the solid volume fractions and solid mass fractions in this work are equal since the densities of all the components in a control volume are the same (because there is no flow between the control volumes).

The conductivities $k_{i-1,i}$ and $k_{i,i+1}$ are evaluated at the interface between control volumes; for example

$$k_{i,i+1} = \overline{SVF}_{i,i+1} \cdot k_{PU}(\overline{T}_{i,i+1}) + (1 - \overline{SVF}_{i,i+1}) \cdot k_{AIR}(\overline{T}_{i,i+1}) \qquad (15)$$

where

$$\overline{T}_{i,i+1} = \frac{T_i + T_{i+1}}{2} \quad \text{and} \quad \overline{SMF}_{i,i+1} = \frac{SVF_i + SVF_{i+1}}{2}. \qquad (16)$$

The heat transfer by radiation between the interior surface of the package skin and the exterior surface of the control volume is calculated only if the SMFs in all the control volumes between those two surfaces are less than 0.038 ($SMF_i < 0.038$). If that is the case, then

$$Q_{RAD} = \frac{2\pi R_{i,Ext}\varepsilon_i\sigma(T_{i,Ext}^4 - T_{S,Int}^4)}{1 + \frac{R_{i,Ext}\varepsilon_i}{R_{S,Int}\varepsilon_S}} \qquad (17)$$

In this expression, $R_{i,Ext}$ is the radius of the exterior surface of volume i, and $R_{S,Int}$ is the radius of the interior surface of the package skin. The emissivities of the outer surface of volume i and the interior surface of the skin are ε_i and ε_S, respectively. The temperatures of these surfaces are $T_{i,Ext}$ and $T_{S,Int}$. The Stefan-Boltzmann constant is σ. In the current work we assume $T_{i,Ext} = T_i$.

A heat flux of 45.8 W/m^2 is applied to the interior surface of the liner to model the heat dissipated by a 19-W payload. A convection coefficient of h = 5 W/m^{2}K and emissivity of ε = 0.1 are applied to the external surface of the skin. A pre-fire calculation is performed in which the environment temperature is set to $T_{ENV} = T_{Normal}$ = 311 K (38°C), and the calculation is run until the system reaches steady state (the average nodal temperatures rate of change is less than $dT_N/dt < 0.001$ K/h). This is used as the initial condition for a fire calculation.

At time t = 0, the environment temperature is set to $T_{ENV} = T_{Fire}$ = 1073 K (800°C), and held there for a fire duration of D_{Fire}. At t = D_{Fire} , the environmental temperature is changed back to the normal value $T_{ENV} = T_{Normal}$ = 311 K. A transient simulation is then performed until $dT_N/dt <$ 0.001 K/h

RESULTS

This section presents five simulated responses of the PU foam during and after fires with temperature T_{Fire} = 1073 K (800°C). In the first four simulations, the fire duration D_{Fire} is 20 hours, which is sufficiently long for the reaction front to reach the package liner. The first two use a normally distributed foam damage model, $z = z_N(\Phi)$ as shown in Figure 3. The first of these is performed with the emissivities of the interior of the package skin and the un-degraded foam exterior both being zero ($\varepsilon_i = \varepsilon_S = 0$), so there is no radiation heat transfer between those surfaces. In the second simulation, those emissivities are set to $\varepsilon_i = \varepsilon_S = 1$ to maximize the effect of surface-to-surface radiation. The results of two more simulations with two different foam

damage models are then presented. The final simulation calculates the response of the package to a regulatory fire of duration D = 0.5 hour.

In all cases, a pre-fire simulation was performed to determine the system temperature and composition profiles in a 311 K (38°C) environment. These results were used as initial conditions for the fire/post-fire simulations.

Normally-distributed damage model

No skin-to-foam radiation. Figure 8 shows time-dependent response characteristics during and after a 20-hour fire with a normally-distributed foam damage model and no skin-to-foam radiation. Figure 8a shows the time-dependence of the environmental temperature T_{ENV}, and the resulting temperature of the outermost and innermost portions of the foam/gas region, T_{OUT} and T_{IN}, respectively. Before the fire begins, the innermost and outer most foam/gas temperatures are, respectively, 103°C (376 K) and 46°C (319 K). The inner temperature is hotter than the outer because the heat flux applied to the interior of the liner, which simulates the payload heat generation.

The environmental temperature is set to 800°C (1071 K) for the first 20 hours of the simulation, then brought down to 38°C (311 K). The outermost temperature increases rapidly after the fire starts and approaches the fire temperature near the end of the fire. It drops off rapidly after the simulated fire is extinguished. The innermost temperature remains essentially constant during the first 2 hours of the fire before a significant amount of heat has transferred to that location. It then rises rapidly, slows down from t = ~9 to 13 hours, and then resumes a rapid rise. The inner temperature continues to rise after the fire is extinguished because heat from the hotter outer portion of the package continues to defuse to that location. The inner temperature peaks at 594°C (867 K) about 2 hours after the fire is extinguished. Long after the fire, the outer temperature reaches its initial, pre-fire value. However, the post-fire steady state inner temperature is 162°C (435 K), which is 59°C hotter than the pre-fire value. This is because the foam was consumed during the fire and replaced with a lower-thermal-conductivity gas.

Figure 8b shows the total masses (per unit length of the package) of the foam, the degraded solid, and the primary and secondary product gases. These amounts are shown versus time only during the 20-hour fire period. Initially, the entire foam/gas region is foam (trace amounts of the other components are also present as a result of the reaction that took place during the pre-fire period). About 6 minutes after the fire begins, the foam mass began to decrease, and it is completely consumed before t = 16 hours. The reaction of the foam produces the primary gas and a smaller amount of degraded solid. The reaction of the degraded solid produces the secondary gas.

The amounts of degraded solid that are produced are small when compared to the amounts of product gases. The degraded solid is completely consumed soon after the foam is consumed. The compositions remain constant after t = 18 hours

Figure 9 shows profiles of temperature versus radial location in the liner, foam/gas, and skin regions. These profiles are shown 1 minute after the fire started (t = 1 min) and at intervals of about 1 hour after that, during the time period when the foam was consumed (see Figure 8b). At time t = 1 min, the interior of the foam/gas region is hotter than the exterior because heat is

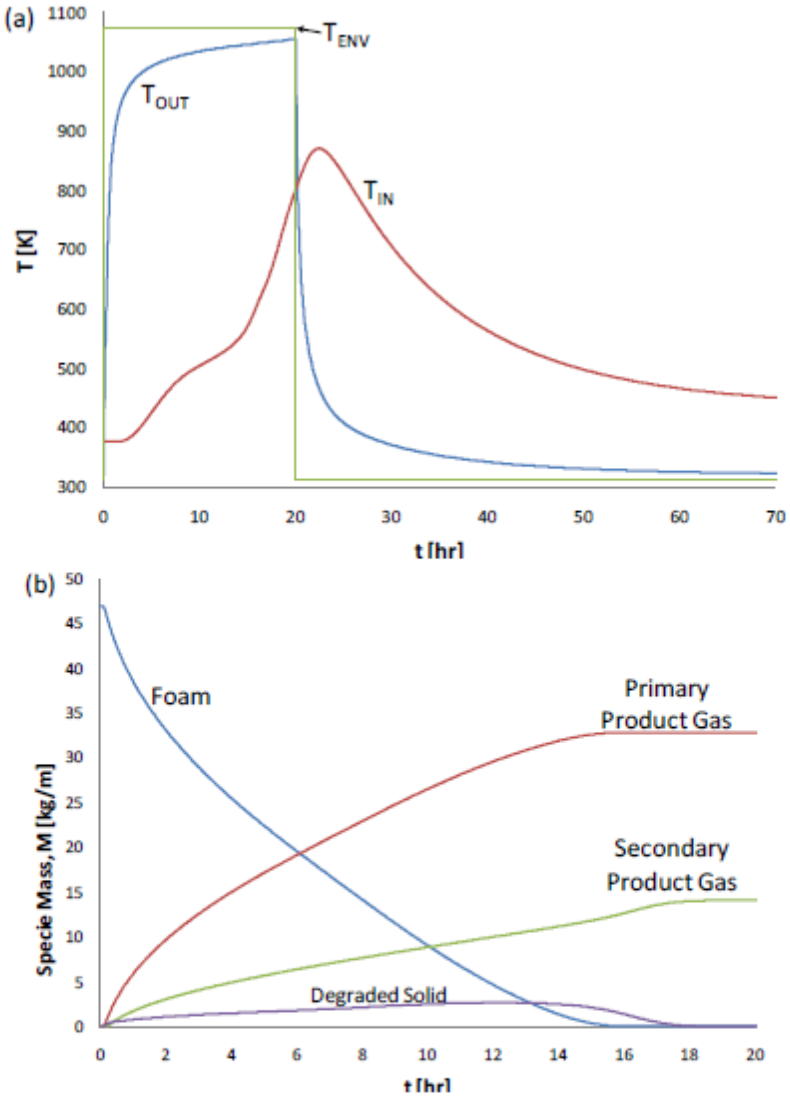

Figure 8 Time-dependent response for $\varepsilon_i = \varepsilon_S = 0$ and the normal damage model during and after a 20-hour, 800°C fire. (a) Environment temperature, outermost PU foam temperature, and innermost foam temperature. (b) Total species mass for all four components

conducting from the liner walls to the edge of the package. The profile has a nearly logarithmic shape because of the cylindrical geometry of the foam/gas region. Once the fire starts, the exterior temperature rises rapidly but the interior changes more slowly. All the profiles have smooth shapes.

Figure 10 shows radial profiles of the properties of the foam/gas mixture at different times. Profiles are shown for t = 1 min and for intervals of about 1 hour after that. Figures 10a and 10b

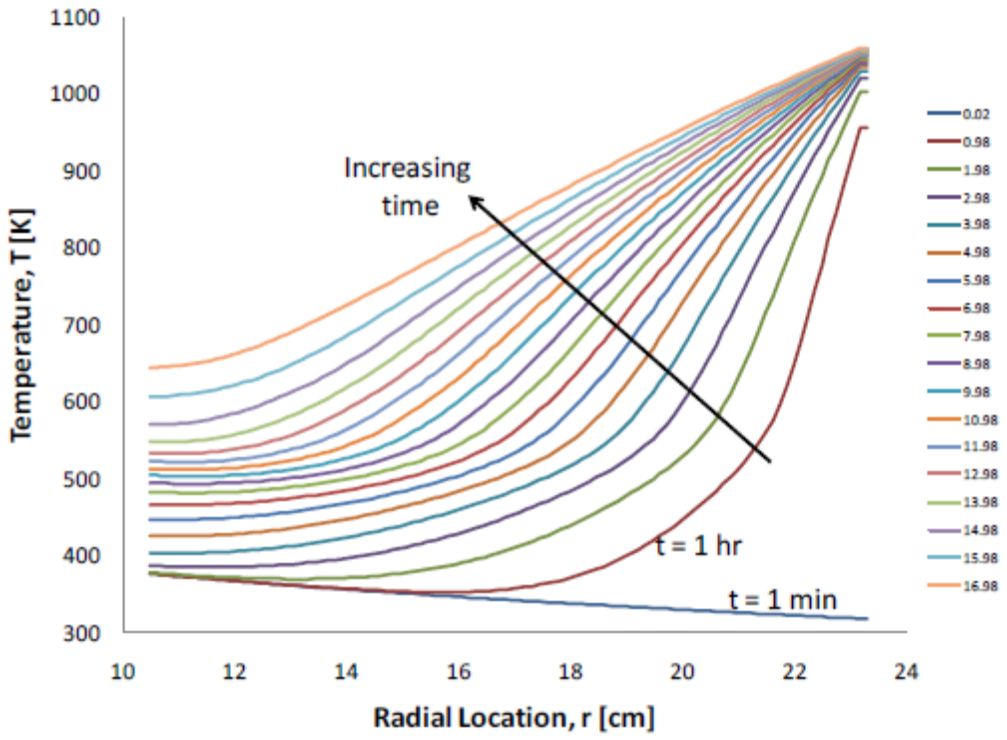

Figure 9 Temperature profiles in foam/gas region, for $\varepsilon_i = \varepsilon_S = 0$ and the normal damage model, while chemical reaction is taking place. Profiles are given at one-hour intervals beginning at time of fire start, t = 1 min.

show profiles of the SMF and mixture thermal conductivity k, respectively. The SMF at the beginning of the fire is one (SMF = 1). Soon after the fire begins the regions near the skin exhibit SMF = 0 (entirely gas) and transition to SMF = 1 (entirely solid) further inside. This transition location moves toward the center of the package as the fire continues. Late in the reaction period the value of SMF decreases near the wall. This is because heat is being conducted to that region from the package payload. This makes the material near the outer edge of the liner hot enough to react and produce gas.

The horizontal dashed line marked SMF = 0.038 shows the value of the solid mass fraction used in the surface-to-surface radiation calculation. Regions with an SMF below this value are clear enough to transmit thermal radiation, while regions with an SMF above it absorb radiation. We see that the region that is clear enough to transmit radiation grows inward from the outer skin as the fire continues. We also note, however, that for the simulation in this subsection, there is no surface-to-surface radiation because $\varepsilon_i = \varepsilon_S = 0$.

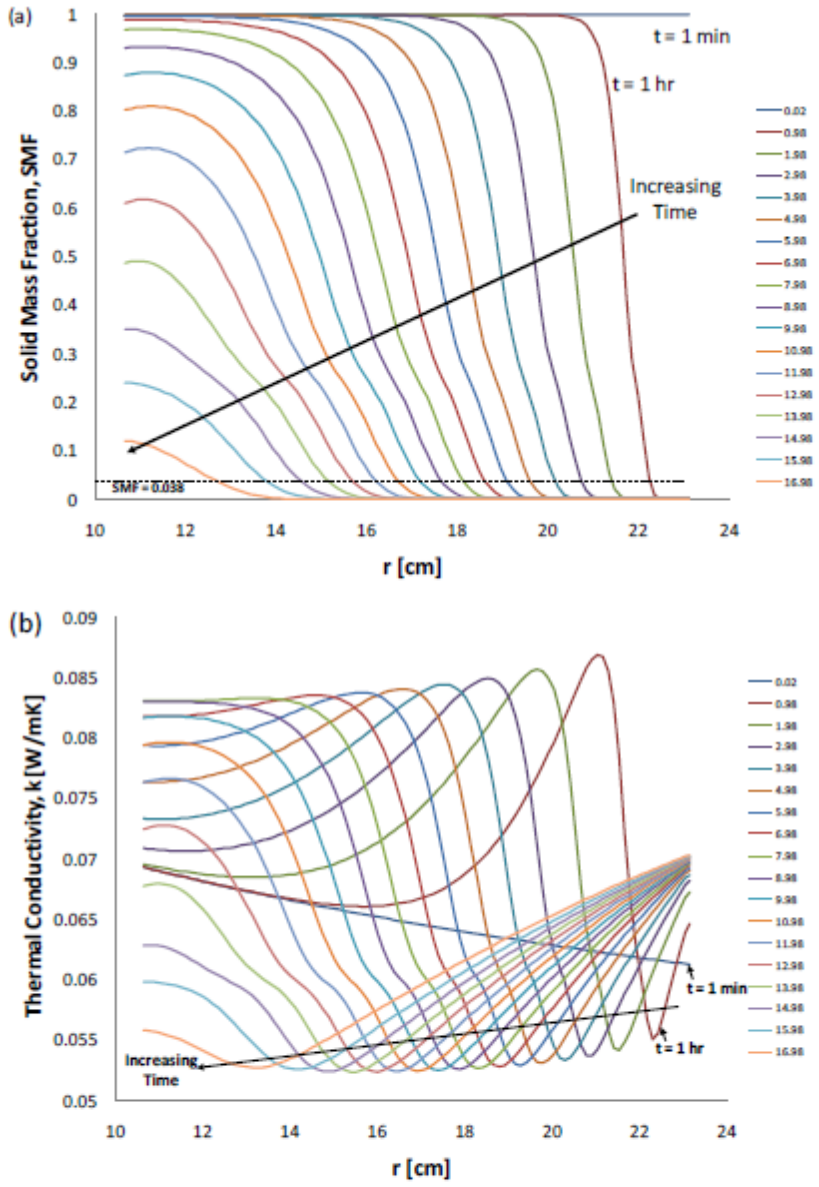

Figure 10 Properties of the foam/gas region, for $\varepsilon_i = \varepsilon_S = 0$ and the normal damage model, while chemical reaction is taking place. Profiles are given at one-hour intervals beginning at time of fire start, t = 1 min. (a) Solid Mass Fraction. (b) Mixture thermal conductivity.

Figure 10b shows profiles of mixture thermal conductivity versus radial location during the reaction period. At t = 1 min, the foam/gas region is entirely foam, and the temperature at the center of the package is greater than that near the edge. The thermal conductivity is higher near the center of the package because the foam thermal conductivity increases with temperature (see Figure 7a). The temperature in the exterior regions of the package increases after the fire starts. This increased temperature first causes the thermal conductivity to increase, but as the solid foam

is consumed and replaced by gas (whose thermal conductivity is less than that of the solid), the mixture's conductivity decreases. The nearly vertical portion of each profile corresponds to the location of the interface between the solid and gas regions. That location moves toward the package center as the reaction continues.

Figure 11 shows profiles of the reaction rate at different times during the reaction period. Results for reaction steps 1 and 2 are shown in Figures 11a and 11b, respectively. At time t = 1 min the reaction rate is essentially zero everywhere. The reaction rate increases in the outer region of the package as the temperature there increases. However, as the reactants are consumed, the reaction rate decreases. The decreased rate leads to spikes that move toward the package center as the fire continues. The primary reaction rate r_1 is significantly larger than the secondary reaction rate r_2.

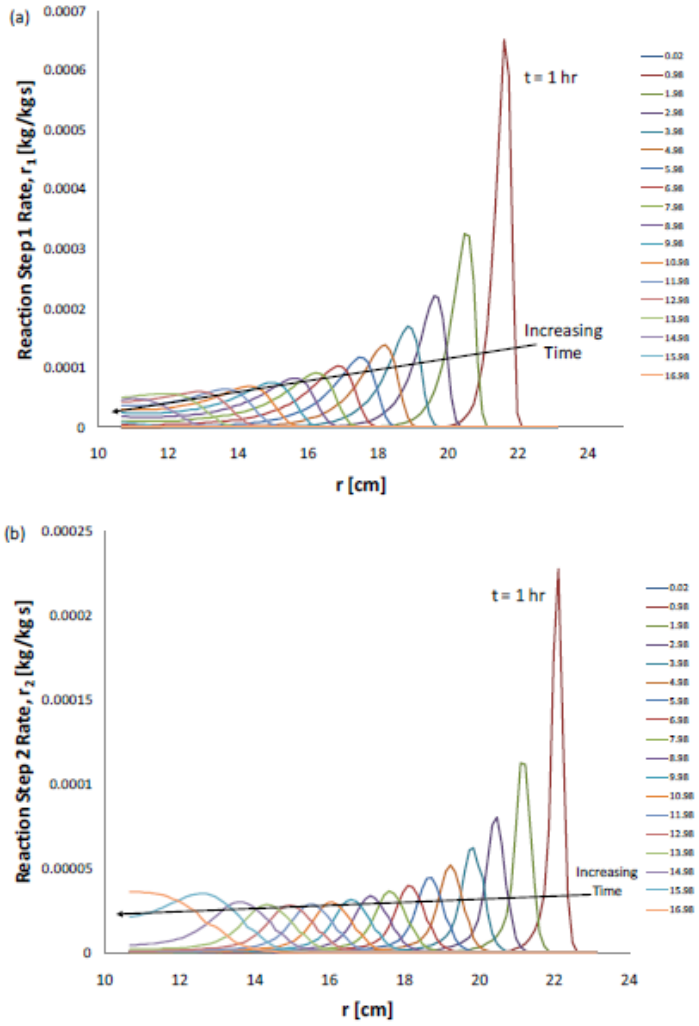

Figure 11 Reaction rate of the foam/gas region, for $\varepsilon_i = \varepsilon_S = 0$ and the normal damage model, while chemical reaction is taking place. Profiles are given at one-hour intervals beginning at time of fire start, t = 1 min. (a) Primary reaction rate. (b) Secondary reaction rate.

Maximum skin-to-foam radiation. This subsection presents results for the maximum possible surface-to-surface radiation between the interior of the package skin and the un-degraded foam, $\varepsilon_i = \varepsilon_S = 1$ (see Equation 17). Comparisons of these results to those of the last section show the possible effects of radiation across the gas-filled region between these surfaces.

Figure 12 shows time-dependent response characteristics during and after the fire, and it can be compared to Figure 8. Figure 12a shows that the environmental temperature is set to 1071 K for the 20-hour fire and then brought down to 311 K. The temperature of the outermost foam/gas region, T_{OUT}, increases rapidly at first, as it did for the simulation for no surface-to-surface radiation. However, during the period t = 0.26 to 2.7 hours, the rate of increase is much less than the no surface-to-surface radiation results. After this period, the outer temperature rises quickly and essentially reaches the fire environmental temperature at t = 10 hours. It drops off quickly after the fire.

The innermost temperature does not respond until about 2 hours after the fire begins, similar to the results for no surface-to-surface radiation in Figure 8a. However, after that time the inner temperature rises much more rapidly than it did in the earlier calculations. This is expected since the heat transfer between the skin and foam surfaces is much greater because a high level of radiation heat transfer is included. The temperatures of the inner and outer regions are nearly identical for the rest of the simulation.

Figure 12b shows the species-mass versus time. While Figure 8b reported results for the full 20-hour fire duration, Figure. 12b shows results for only 4 hours. When surface-to-surface radiation is included the foam is completely consumed in just 2.9 hours compared to 16 hours when it is excluded. This is because the rate of heat transfer from the skin to the foam is enhanced because radiation is included. Radiation allows the region of the foam that is reacting to be in direct thermal contact with the hot package skin. Since the reaction zone is cooled by the endothermic process, this removes heat from the skin. This is why the outer edge of the foam/gas region (T_{OUT} in Figure. 12a) is cooler during the period t = 0.26 to 2.7 hours for the current high surface-to-surface radiation calculation than it was for the no radiation heat transfer calculation in the last subsection.

Figure 13 shows temperature profiles in the skin, foam/gas and liner regions at different times during the reaction period. The profiles in Figure 13 are given at t = 1 min and t = 5 min and at 10 min intervals after that. The profiles are much less smooth than they are in Figure 9. High levels of radiation heat transfer across the gas-filled region cause that region to be nearly isothermal. There are much larger gradients in the solid foam regions interior to the gas.

Effect of Damage Model

In the last section, the normally-distributed damage model was used to calculate the distribution variable z and the resulting reduction in the thermal degradation rate as the reaction extend Φ increased. Those results indicate that the solid foam in the outer portion of the foam/gas region is replaced by product gases that allow radiation from the outer skin to be transmitted to the un-degraded foam. Depending on the effective emissivities of the foam and skin surfaces, the foam is completely consumed after fire exposure that lasted between 2.9 and 16 hours.

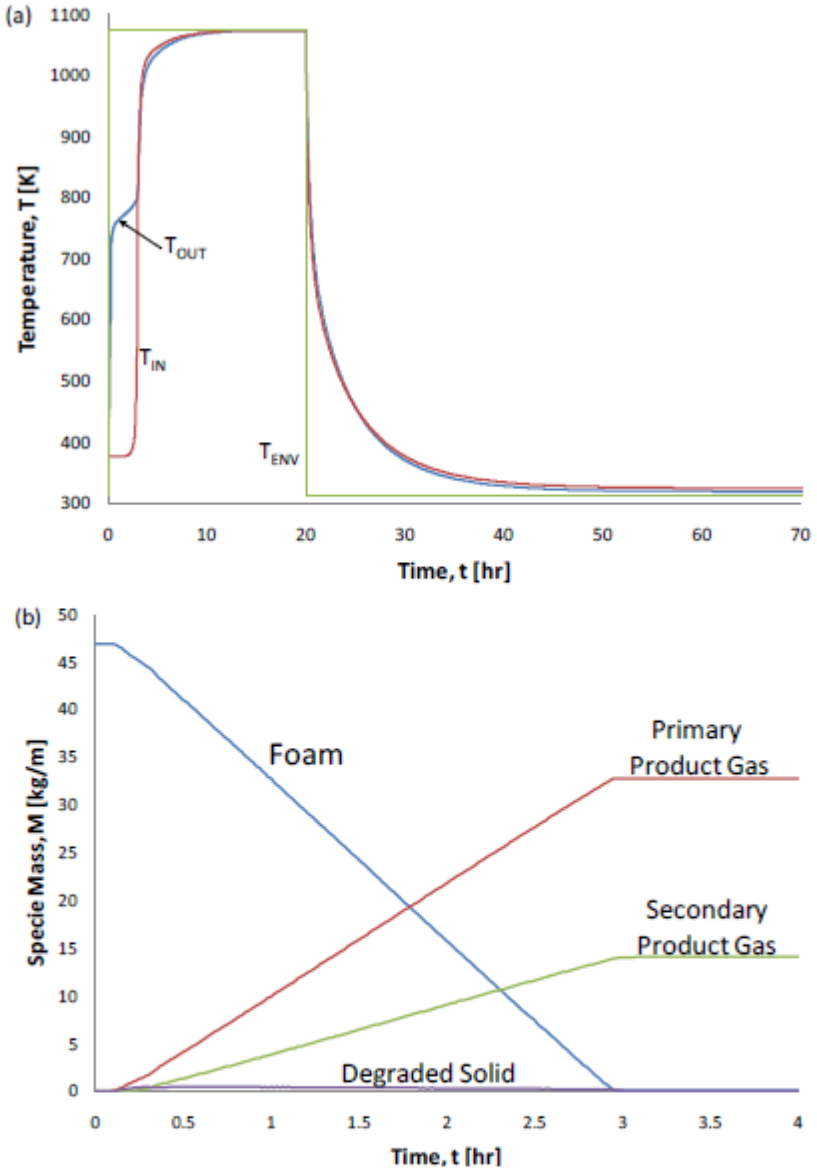

Figure 12 Time-dependent response for $\varepsilon_i = \varepsilon_S = 1$ and the normal damage model during and after a 20-hour, 800°C fire. (a) Environment temperature, outermost PU foam temperature, and innermost foam temperature. (b) Total species mass for all four components

Figure 3, which was discussed earlier, shows a 9977 package after a 30-min fire test. It shows that the PU foam in the outer region was replaced by a layer of visually opaque char, not a clear gas. This suggests that the normal foam damage model used in the last section may not sufficiently reduce the degradation reaction rate.

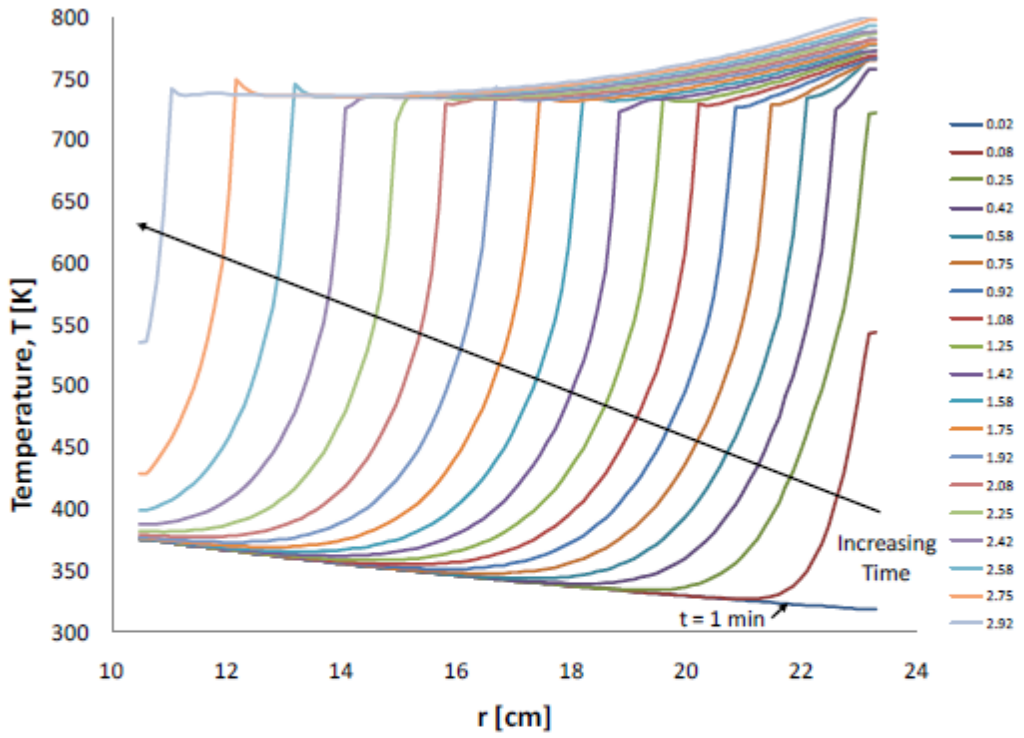

Figure 13 Temperature profiles in foam/gas region for $\varepsilon_i = \varepsilon_S = 1$ and the normal damage model, while chemical reaction is taking place. Profiles are given at times t = 1 and 5 min, and then 10-minute intervals thereafter.

In this section we present results from simulations with two different foam damage models. In the first, the distribution variables are set to $z_1 = z_2 = 0$. Comparing that result with the results in the last section shows the effect of the normal damage model ($z = z_N(\Phi)$). In the second damage model, the distribution variable is calculated as $z = z_N(\Phi+0.04)$, which is shown in Figure 3 as the line marked "Shifted." This model causes the reaction to slow down and essentially stop when the reaction extent Φ approaches 0.96 and the SMF within a control volume is roughly 0.04. The shift value of 0.04 was chosen because it keeps the SMF at all locations above 0.038, which is the value used in the current work to allow radiation to be transmitted through a control volume. Future work should measure the density of the char foam product after the fire to derive a more rationally-based shift value.

No reaction damage. The time-dependent response and temperature profiles from simulations that use $z_1 = z_2 = 0$ and $\varepsilon_i = \varepsilon_S = 1$ are qualitatively similar to the simulation results from the normal damage model shown in Figures 12 and 13. Plots of the no-damage model results are therefore not included in this paper. However, when the no-damage model is used, the foam is consumed (F = 0) in 2.6 hours compared to 2.9 hours when damage is included (Figure 12b). In the normal damage model, the consumption of foam is slowed down from that in the no-damage

model ($z_1 = z_2 = 0$). However, as mentioned earlier, this model does not predict that a layer of char will remain within the foam/gas region after the fire is extinguished.

Shifted damage model. Figure 14 shows time-dependent response characteristics during and after a 20-hour fire from a simulation that uses the shifted damage model. Even though this simulation includes skin-to-foam radiation ($\varepsilon_i = \varepsilon_S = 1$), the results are more similar to those presented in Figure 8 for the normal damage model with zero surface-to-surface radiation ($\varepsilon_i = \varepsilon_S = 0$) than they are to the results with radiation presented in Figure 12.

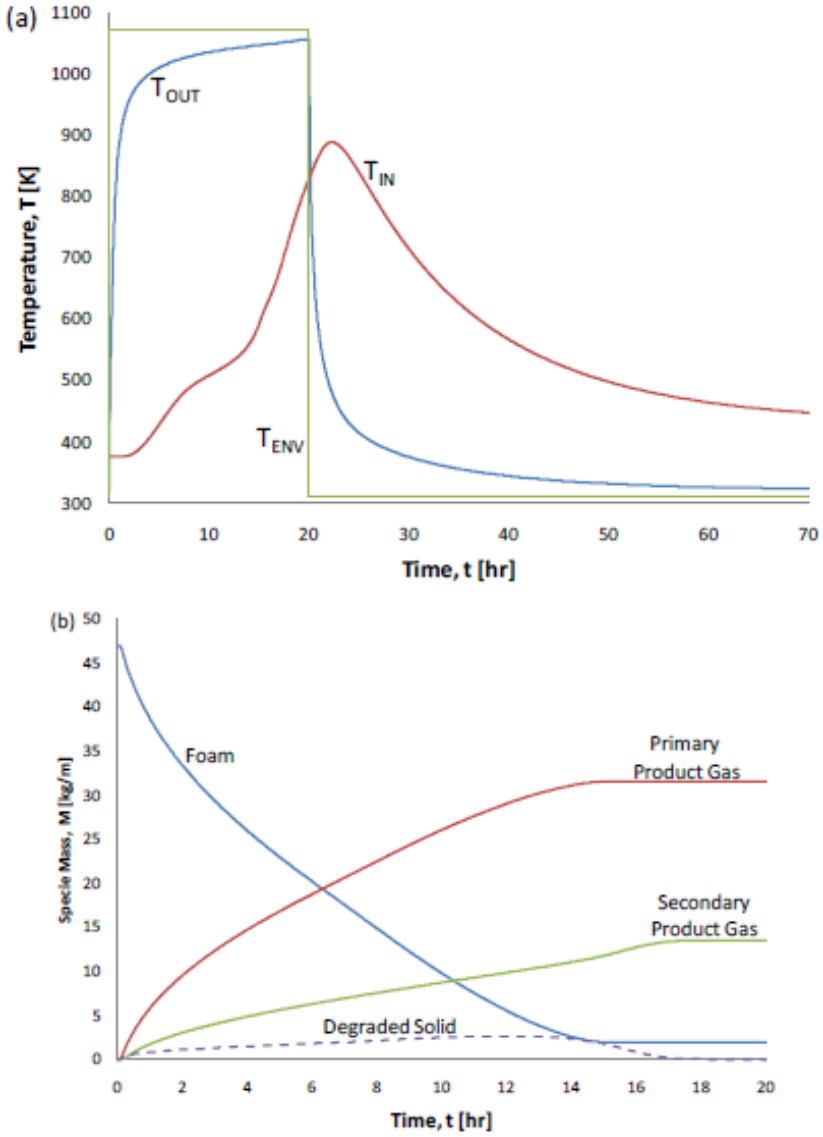

Figure 14 Time-dependent response for the shifted damage model and $\varepsilon_i = \varepsilon_S = 1$ during and after a 20-hour, 800°C fire. (a) Environment temperature, outermost PU foam temperature, and innermost foam temperature. (b) Total species mass for all four components

The species mass versus time behavior in Figure 14b is similar to that in Figure 8b for the first 12 hours of the fire. However, the shifted damage model caused the consumption of foam to essentially stop after that time. The degraded solid is consumed shortly after that, and then the composition remains constant. The peak interior temperature for the normal damage model in Figure 8a is T_{IN} = 864 K, but that temperature is 18 K higher in Figure 14a when the shifted damage model is used.

There are two reasons for this. The first is that foam remains in the domain and its thermal conductivity is higher than that of the gas. The second is that the foam consumption reaction is endothermic. Since less foam is consumed, less sensible energy is removed from the system.

Figure 15 shows profiles of the SMF during the foam consumption period. When the shifted material damage model is used, after sufficient time, the foam/gas region is filled with a mixture whose SMF is 0.041 (it was zero for the normal damage model in Figure 10a). Another simulation performed that minimized the effect of surface-to-surface radiation ($\sigma_1 = \sigma_2 = 0$) gave identical results to those of Figures 14 and 15. This is because, whenever the shifted damage model is used, the SMF never drops below 0.038, the value that allows radiation transmission.

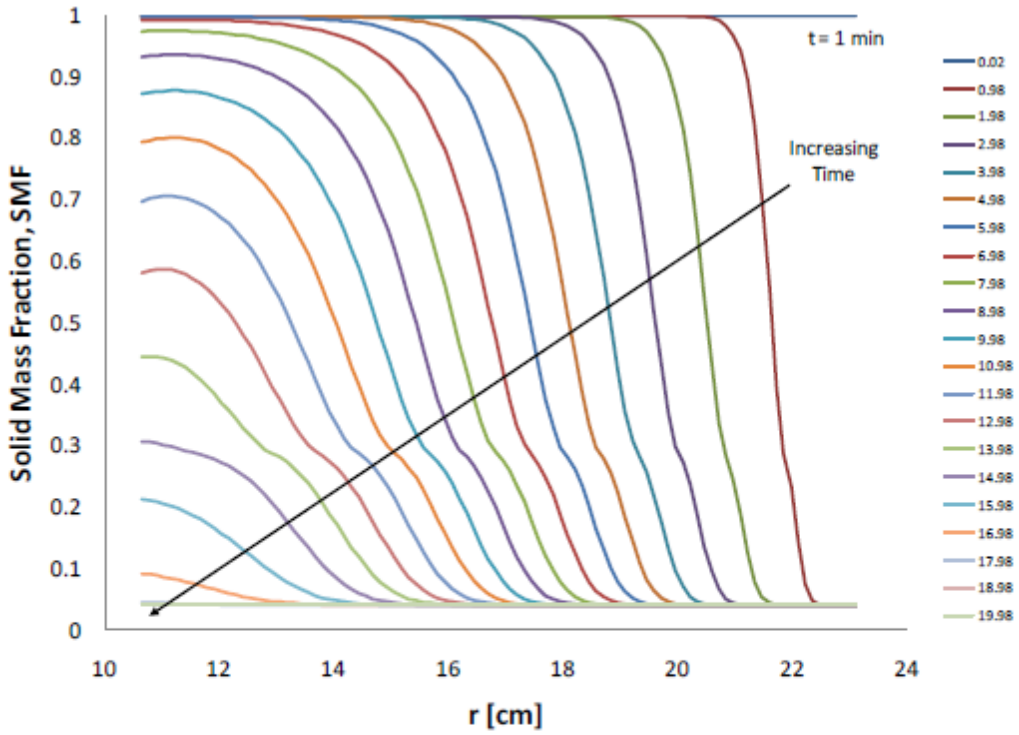

Figure 15 Profiles of solid mass fraction versus radial location for the shifted damage model and $\varepsilon_i = \varepsilon_S = 1$, while chemical reaction is taking place. Profiles are given at t = 1 min and one-hour intervals thereafter.

Regulator Fire Duration

Figure 16 shows time-dependent response characteristics during and after a fire with the regulatory duration of only D_{FIRE} = 30 min. This simulation used the shifted damage model. The peak inner and outer foam/gas temperatures in Figure 16a are 129°C (402 K) and 482°C (755 K), respectively. The inner temperature is well below the value for the limit for short-term (fire) conditions for the containment vessel seal, 377°C (700°F).

Figure 16b shows that only a small fraction of the foam is consumed during a 30-min fire. The composition within the foam/gas does not change appreciably after t = 0.8 hour. In the earlier simulations with fire durations of D_{FIRE} = 20 hours, the steady-state composition had no degraded solid. However, degraded solid is part of the steady-state composition for the D_{FIRE} = 0.5-hour fire.

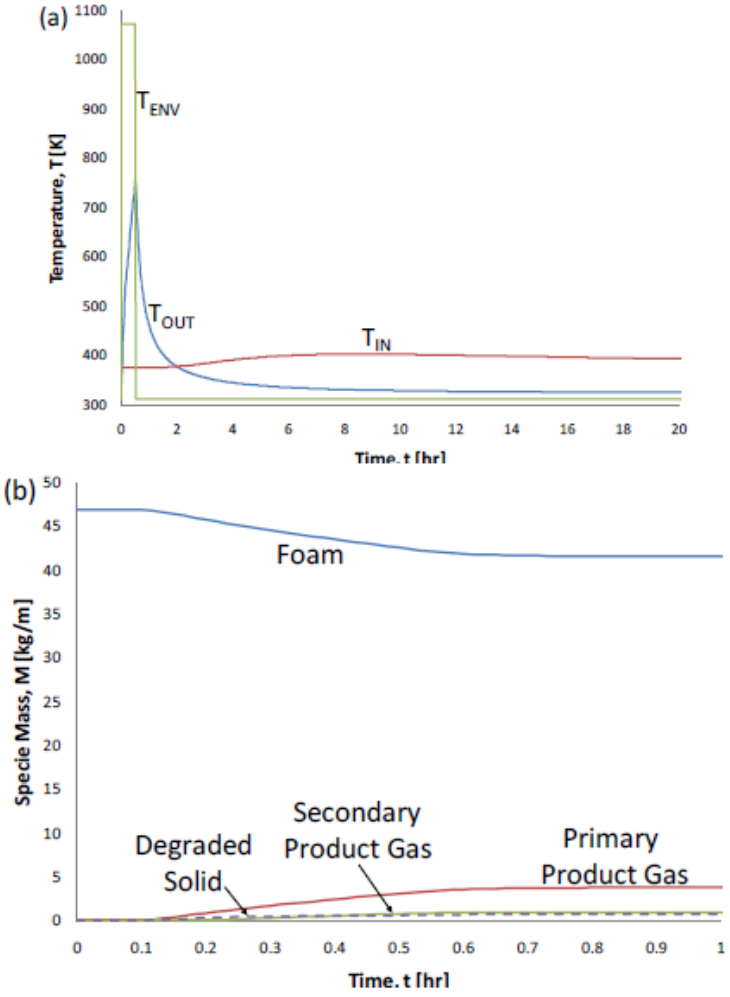

Figure 16 Time-dependent response for the shifted damage model and $\varepsilon_i = \varepsilon_S = 1$ during and after a 30-minute, 800°C fire. (a) Environment temperature, outermost PU foam temperature, and innermost foam temperature. (b) Total species mass for all four components

CONCLUSIONS

Polyurethane foam is used in the annular region between the inner liner and the outer skin of 9977 drum packages to assure package integrity during impact and fire events. In this work, a one-dimensional axis-symmetric finite difference model is developed to calculate the temperature and composition within the foam region caused by 800°C fires. This model includes radiation and convection heat transfer between normal or fire environments and the external package skin. It uses a mass-based chemical kinetics model (developed by other investigators) to predict the rate of foam consumption as well as product gas, degraded solid and heat generation. The model calculates transient conduction in the skin, liner, and annular region containing the foam and gas products. The specific heat and thermal conductivity of the foam/gas mixture are calculated as functions of its temperature and composition. The effect of surface-to-surface radiation through the low SMF region between the package skin and the un-degraded foam is included.

The decomposition reaction rate is determined as a function of the local temperature, and is reduced on the basis of the cumulative material damage caused by the reaction. Results calculated by using a normally-distributed damage model are compared to results from a "shifted" damage model developed in this work.

Simulations were performed for a 20-hour fire. If the normal material damage model is employed, a gas-filled region develops near the package skin as the foam is consumed. This region is clear enough to allow thermal radiation between the package skin and un-degraded foam. Depending on the effective emissivities of the un-degraded foam and skin surfaces, the foam is completely consumed after fire exposure lasting between 2.9 and 16 hours. However, fire tests show that the PU foam in the outer region is replaced by a layer of visually opaque char, not a clear gas. This suggests that the normally distributed foam damage model may not sufficiently reduce the degradation reaction rate.

The shifted material damage model developed in this work slows down and stops the reaction at locations where the SMF is roughly 4%. Because the solid foam lattice is not completely consumed, there is no direct thermal radiation between the package skin and the reacting zone of the foam. As a result, this process is not affected by the emissive properties of the skin and un-degraded foam.

A simulation that used the shifted material damage model was performed for a 30-min regulatory fire. The peak temperature of the inner liner reached 129°C, which is well below the short-term (fire) conditions limit for the containment vessel seal of 377°C (700°F).

The current model does not include the effect of gas or degraded foam flowing out of the domain. The value of the SMF that causes the reaction to stop (4%) was chosen somewhat arbitrarily. Future work should incorporate the effect of the flowing materials. It should also include measurement of the density of the degraded material that remains after fire tests to determine a more rationally-based value of the reaction-stop SMF. Once these improvements have been made, the resulting model can be used (a) to predict the amount of time combustible gas will flow out of a package during and after a fire, and (b) to design the thickness of PU foam layers used to protect packages during fire events.

ACKNOWLEDGMENTS
This work was supported by the U.S. Department of Energy's Faculty Sabbatical Program, through the Division of Educational Programs at Argonne National Laboratory, under contract DE-AC02-06CH11357.

REFERENCES

1. U.S. Nuclear Regulatory Commission, 2009, "Packaging and Transportation of Radioactive Material," Code of Federal Regulations, 10 CFR 71, Washington, DC.

2. Fluor Hanford, Inc., 2008, *Hanford Unirradiated Fuel Package (HUFP) Safety Analysis Report for Packaging (SARP)*, HNF-28554, Rev. 1, Richland, WA, May.

3. Savannah River Packaging Technology, 2006, "Safety Analysis Report for Packaging Model 9977," S-SARP-G-00001, Washington Savannah River Company, Savannah River Site, Aiken, SC.

4. Williamson, C.L., and Iams, Z.L., 2004, "Thermal Assault and Polyurethane Foam Evaluating Protective Mechanisms," presented at *Packaging and Transport of Radioactive Materials (PATRAM), Berlin, Germany*.

5. Li, J., Tam, S.W, and Liu, Y.Y., 2009, "Burn Behavior of a Polyurethane Foam Impact Limiter," PVP2009-77261, presented at 2009 ASME Pressure Vessels and Piping Division Conference, Prague, Czech Republic, July 26–30.

6. Smith, A.C., Gelder, L.F., Blanton, P.S., and Lutz, R.N., 2005, "Performance of a Drum Type Packaging with Urethane Foam Overpack Subjected to Crush and Other Regulatory Tests," PVP2005-71033, presented at Transportation, Storage and Disposal of Radioactive Materials, Denver, CO, July 17–21.

7. Smith, A.C., May, C.G., Blanton, P.S., Abramczyk, G.A., Gelder, L.F., and Malloy, J.D., 2006, "The General Purpose Fissile Package, A Replacement for the 6M Specification Package," WSRC-MS-2006-00030, presented at Institute of Nuclear Materials Management Conference.

8. Hobbs, M.L., and Lemmon, G.H., 2003, "SPUF – A Simple Polyurethane Foam Mass Loss and Response Model," Report SAND2003-2099, Sandia National Laboratories.

9. Hobbs, M.L, and Lemmon, G.H., 2004, "Polyurethane Foam Response to Fire in Practical Geometries," *Polymer Degradation and Stability*, Vol. 84, pp. 183–197.

10. Bejan, A., 2004, *Convection Heat Transfer*, 3rd Edition, John Wiley & Sons, Hoboken, NJ